Effects of Addition of Acrylic Compatibilizer on the Morphology and Mechanical Behavior of Amorphous Polyamide/SAN Blends

D. Becker,[1] E. Hage Jr.,[2] L. A. Pessan[2]

[1]*Materials Science and Engineering Graduate Program, Universidade Federal de São Carlos, São Carlos, 13565-905 SP, Brazil*
[2]*Department of Materials Engineering, Universidade Federal de São Carlos, São Carlos, 13565-905 SP, Brazil*

Received 4 December 2006; accepted 28 July 2009
DOI 10.1002/app.31238
Published online 15 October 2009 in Wiley InterScience (www.interscience.wiley.com).

ABSTRACT: Amorphous polyamide (aPA)/acrylonitrile-styrene copolymer (SAN) blends were prepared using methyl methacrylate-maleic anhydride copolymer MMA-MA as compatibilizer. The aPA/SAN blends can be considered as a less complex version of the aPA/ABS (acrylonitrilebutadiene-styrene) blends, due to the absence of the ABS rubber phase in the SAN material. It is known that acrylic copolymer might be miscible with SAN, whereas the maleic anhydride groups from MMA-MA can react *in situ* with the amine end groups of aPA during melt blending. As a result, it is possible the *in situ* formation of aPA-g-MMA-MA grafted copolymers at the aPA/SAN interface during the melt processing of the blends. In this study, the MA content in the MMA-MA copolymer and its molecular weight was varied independently and their effects on the blend morphology and stress–strain behavior were evaluated. The morphology of the blends aPA/SAN showed a minimum in the SAN particle size at low amounts of MA in the compatibilizer, however, as the MA content in the MMA-MA copolymer was increased larger SAN particle sizes were observed in the systems. In addition, higher MA content in the compatibilizer lead to less ductile aPA/SAN blends under tensile testing. The results shown the viscosity ratio also plays a very important role in the morphology formation and consequently on the properties of the aPA/SAN blends studied. © 2009 Wiley Periodicals, Inc. J Appl Polym Sci 115: 2540–2549, 2010

Key words: amorphous polyamide; acrylic compatibilizer; SAN; polymer blends

INTRODUCTION

Much attention has been paid to the use of reactive compatibilizer in immiscible polymer blends for controlling phase morphology and improving mechanical properties in a variety of systems.[1–5] Usually, the potential reactive compatibilizer used has specific functional groups which can generate *in situ* formation of block or graft copolymers at the interface region during the blend preparation. The *in situ* formed copolymer at the interface usually provides finer morphology and increases the interfacial adhesion strength.[1]

When selecting a compatibilizing agent for a given polymer blend, it is necessary to consider its characteristics like chemical composition, molecular weight, and molecular architecture. Thus, it is necessary to understand the effects of molecular parameters of these copolymers on their ability for compatibilizing the polymer system under study. Larocca et al.[6] have observed the compatibilization effects of methyl methacrylate-glycidyl methacrylate (MGE) copolymer on the PBT/AES/MGE blends, where low-molecular-weight MGE grades are more efficient.

Maleic anhydride (MA)-modified polymers are often used as compatibilizers in blends with polyamide due to the high probability of chemical reaction between MA functional unities and the amine end-groups of polyamide (PA) during melt blending.[7–10] This reaction is expected to take place fast and results in imide linkage formation, as shown in Figure 1. Usually, this imide linkage is formed at the polyamide blend interface, thereby leading to adequate blend compatibilization. PA/ABS blends have been compatibilized by maleated acrylic copolymers.[11,12] In these systems, the MA groups of MMA-MA molecules react *in situ* with the amine end groups of the PA chains, whereas the MMA copolymer segments form a miscible system with the SAN phase of ABS, promoting adequate interfacial adhesion between PA and ABS.[13–17] The MMA-based copolymers are miscible with SAN within a wide range of AN content in the SAN.[18,19] Due to this fact, MMA-MA copolymers has being used

Correspondence to: L. A. Pessan (pessan@ufscar.br).
Contract grant sponsors: CNPq, FINEP/PRONEX-Brazil, FAPESP.

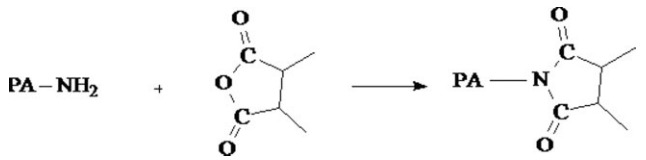

Figure 1 Scheme of interface grafting by reaction between a carboxyl group of maleic anhydride and a polyamide amino end group.

successfully as a compatibilizer for polyamide and SAN-based polymer blends.[12,20]

The aim of this work was to gain insights on how MMA-MA copolymers with different molecular weight and MA content affects the morphology and mechanical properties of the amorphous PA/SAN blends and contribute to the understanding about the behavior of more complex systems such as aPA/ABS and PA/ABS.

EXPERIMENTAL

Materials

The chemical structure of the amorphous polyamide used in this study is illustrated in Figure 2. This material was supplied by DuPont and is commercialized as SelarPA 3426. The SAN material used was supplied by DOW Chemical as Tyrill 790. The characteristics of these materials are shown in Table I.

Synthesis of the compatibilizer

The MMA-MA copolymers used in this study were synthesized by solution polymerization, using methyl methacrylate (MMA) and maleic anhydride (MA) as comonomers, as well as, ethyl acrylate (EA) as auxiliary comonomer to increase the thermal stability of the copolymer against unzipping thermal degradation.[6] The polymerization reaction was carried out in a reactor under intensive mixing and nitrogen atmosphere at 80°C for 8 h. The copolymers were synthesized with 1, 5, and 10 wt % of MA, using toluene as solvent. To control the molecular weight of the copolymers, the initiator benzoil peroxide was used at different concentrations as follows: for high-molecular-weight (HMW) 1% of peroxide; for medium-molecular-weight (MMW) 2% of peroxide; and for low-molecular-weight (LMW) 5% of peroxide. The volume of solvent in the reactor was kept constant to maintain the monomers concentration at 2 g/mol. The copolymer obtained through the polymerization reaction was then fractionated by precipitation in methanol at 1 : 10 v/v ratio, to remove all toluene and nonreacted maleic anhydride. The synthesis technique used in this study was a modified procedure based on similar reactions reported in the literature.[21–23] The copolymer MMAMA was characterized by gel permeation chromatography (GPC) and titration, and the results are presented in Table II.

Evidences for *in situ* reactions during melt blending

A Haake torque rheometer, model RHEOMIX 600, was used to obtain evidences of *in situ* reactions between aPA and MMA-MA during melt mixing. An increase in the torque values for the blend above the individual ones for each component, during melt mixing, would show evidence for grafting and/or crosslinking reactions in the aPA/MMA-MA blends. The mixture was carried out at 260°C and 60 rpm, in a 69 cm^3 chamber filled upto 70% of its volume. Both components in the powder form were mixed before being added into the chamber.

Blend preparation and compounding

The neat aPA and SAN materials were cryogenically ground into powder and dried for at least 24 h in a vacuum oven at 80°C. The powder materials were then thoroughly mixed and melt-compounded in a corotating twin-screw extruder Werner & Pfleiderer, model ZSK-30, operated at 150 rpm, with a flat temperature profile along the barrel (260°C). The aPA/SAN blend composition studied was 80 wt % of aPA and 20 wt % of SAN. For the ternary blends aPA/SAN/MMA-MA, it was used the composition at the 76/19/5 wt % ratio. The blends prepared were dried in a vacuum oven for 24 h at 80°C before injection molding in an Arburg model 270V injection-molding machine to obtain specimens for tensile tests according to ASTM D638. The injection molding was carried out with a temperature of 250°C in the nozzle and 80°C in the mold.

Dielectric relaxation spectroscopy

Thin samples of the blend SAN/MMA-MA with thickness in the range of 30–60 μm were prepared for dielectric analysis through compression molding at 200°C. Dielectric relaxation experiments were performed using a impedance analyzer Mod. 4192A (Impedance and Gain Phase Analyzer 4192A – HP) in the frequency range of 1–1000 kHz and temperature range between 20 and 180°C.

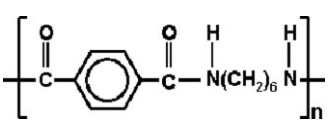

Figure 2 Illustration of the chemical structure of amorphous polyamide used in this study.

TABLE I
Characteristics of the Materials Used in this Study

Materials	Description	Composition	Molecular weight (g/mol)	T_g (°C)
aPA	SelarPA 3426	End group content: $[NH_2]$ 37 × 10^{-6} eq g^{-1}	$\overline{M}_n$ = 12,000 $\overline{M}_w$ = 47,000	127
SAN	Tyrill 790	S = 72% AN = 28%	$\overline{M}_n$ = 61,028 $\overline{M}_w$ = 136,756	110

Transmission electron microscopy

The morphology of the blends was observed through transmission electron microscopy (TEM), using a Jeol 100CX microscope, operating at 80 kV of accelerating voltage.

The samples analyzed by TEM were taken from the injection-molded tensile test specimen. The observed area was located at an intermediary position of thickness and length of the sample and in the direction perpendicular to the injection flow. The samples were stained by immersion in a 10% phosphotungstic acid (PTA) aqueous solution for 6 days, when the substance etches preferably the polyamide phase. After that, the samples were microtomed, i.e., cut into ultrathin sections with nominal thickness of 20 nm on a Leica ultramicrotome using a diamond knife at room temperature. The slices of the polymer samples floating in water both in the ultramicrotome were collected with cooper grids.

Titration

The amorphous polyamide amine end group content, in the blends, was determined by potentiometric titration technique. First, the blend was dissolved in a phenol solution and then the pH turning was determined while adding a 0.1*N* HCl solution. All aPA blends were analyzed for residual amine concentration to measure the extent of reaction, assuming the dominant reaction is between amine and anhydride units to form imide linkages.

TABLE II
Molecular Characteristics of the MMA-MA Copolymers Synthesized

Copolymer	MA content (wt % by titration)	$\overline{M}_n$ (g/mol)	$\overline{M}_w$ (g/mol)	$\overline{M}_n/\overline{M}_w$
MMA-MA1 HMW	1.1	30,729	52,386	1.6
MMA-MA5 HMW	5.0	29,398	57,474	2.0
MMA-MA10 HMW	9.8	23,408	60,365	2.6
MMA-MA1 MMW	0.8	19,779	34,217	1.7
MMA-MA5 MMW	5.1	19,253	33,782	1.8
MMA-MA10 MMW	8.9	15,636	42,839	2.7
MMA-MA1 LMW	0.7	12,364	22,895	1.8
MMA-MA5 LMW	5.9	9262	25,185	2.7
MMA-MA10 LMW	8.2	8081	22,643	2.8

Mechanical testing

Tensile tests, according to the ASTM D638 standards, were carried out in an Instron universal testing machine model 5569, using Type I specimens. Crosshead displacement rate of 5 mm min^{-1} was used. A longitudinal strain gage with 25-mm gap was used to obtain Young modulus.

RESULTS AND DISCUSSION

Evidences for the reaction of compatibilization *in situ*

Figure 3 shows evidences for the reaction between end groups of the aPA and anhydride groups of the MMA-MA copolymer under melt blending in a torque rheometer. All samples show a very intense torque peak at short times of mixing due to the melting process, and then show a tendency to level off at lower torque values for longer mixing times. The MMA-MA samples showed the lowest torque values, whereas neat aPA shows higher torque than MMA-MA copolymer. Samples of poly(methyl methacrylate) (MMA-MA0HMW) were synthesized at the same conditions as the MMA copolymers containing different MA content. The aPA/MMA-MA0HMW blend was used as reference to show the effect of

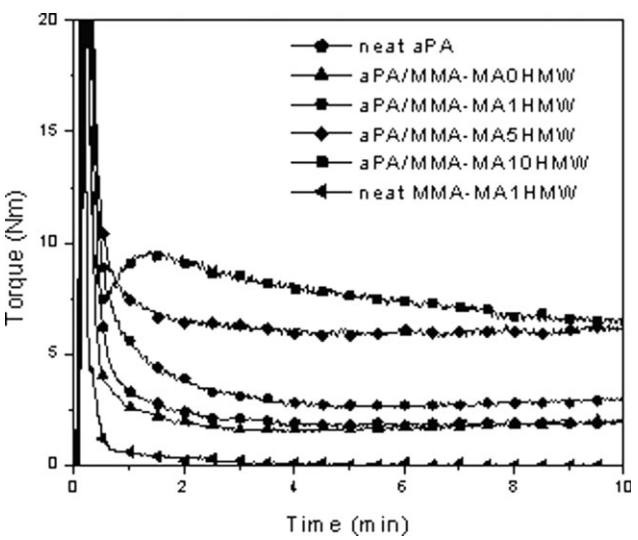

Figure 3 Torque vs. time for aPA/MMA-MA mixtures at 260°C and 60 rpm.

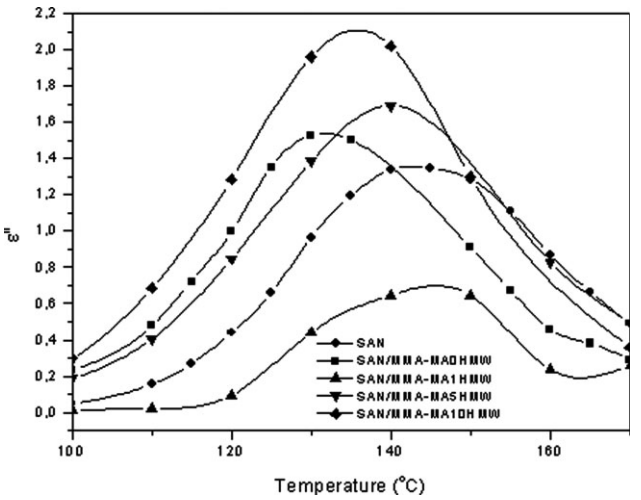

Figure 4 Comparison plot of dielectric loss at 50 kHz versus temperature for SAN/MMA-MA.

presence of MA in the acrylic copolymer for *in situ* reactions with aPA during melt mixing. The torque vs. time curve for aPA/MMA-MA0HMW (80/20) blend show torque values intermediate between the torque values for aPA and for the plain MMA-MA1HMW (Fig. 3), whereas all aPA/MMA-MA blends containing MA in the MMA-MA show torque values above the ones for plain aPA. This behavior shows evidences for the occurrence of grafting reactions between aPA and MMAMA molecules, which leads to higher molecular weights species. As the MA content in the MMA-MA copolymer was increased, the torque levels became higher, which correlates with the higher intensity of the grafting reactions. Almost all aPA/MMA-MA blends with MMA-MA copolymer containing 5 and 10 wt % of MA, for all the molecular weight studied, have shown another torque peak after melting. This effect might be a result of crosslinking reactions followed by thermo-mechanical degradation represented by the decrease in the torque after reaching the maximum torque at the melt state. Considering that most of the aPA/MMA-MA/SAN blends would not have a residence time longer than 2 min during its preparation by melt extrusion, the observed torque peak values are within the residence time needed for the reactive compatibilization in those blends to occur.

Study of the miscibility of SAN/MMA-MA blends

The influence of the MA content in the MMA-MA copolymer on the miscibility between SAN and MMA-MA was studied by dielectric relaxation spectroscopy. Figure 4 shows the dielectric loss (ε'') versus temperature for the SAN/MMA-MA blend at 50 kHz. The neat SAN presents only one relaxation peak which is related to its glass transition temperature ($T_g \sim 143°C$). The addition of MMA to the SAN leads to a shift in the glass transition and only one relaxation peak near 132°C is observed. This observation is a evidence of the miscibility between these SAN and MMA materials. The results of the dielectric relaxation spectroscopy analysis for the SAN/MMA-MA systems with different maleic anhydride content also show only one relaxation peak.

Table III shows the values of activation energy to the relaxation process for the SAN and the SAN/MMA-MA mixtures. The activation energy was calculated by Arrhenius equation (1)

$$f_m = A \exp\left(\frac{-E_a}{RT}\right) \quad (1)$$

where E_a (kJ/mol) is the activation energy, f_m is the peak frequency, and A is the fitted parameter. The slope of the line for the best fit through the $\ln(f_m)$ versus $1/T$ can be used to calculate the activation energy.[24] The SAN/MMA-MA systems present higher activation energy than neat SAN which is related to a lower mobility of polymeric chain in the SAN/MMA-MA system due to the miscibility between SAN and MMA-MA.

aPA/SAN blends morphology

It has been shown in the literature that the presence of adequate copolymers at the interfase of immiscible polymer blends promotes a decrease in the disperse phase particle size, mainly because of the efficiency of these copolymers in promoting a steric stabilization of the disperse particles against the coalescence phenomena.[25–29] The SEM photomicrographs for the binary aPA/SAN and ternary aPA/SAN/MMA-MA blends are shown in Figure 5. As expect, for all blends, the SAN particles are dispersed in the aPA continuous phase. Figure 5(a) shows the morphology for the aPA/SAN binary blend where it can be observed SAN particles with very different sizes. Addition of MMA-MA containing 1 wt % of maleic anhydride (MMA-MA1) seems to promote a reduction in the overall SAN particle

TABLE III
Activation Energy for the SAN/MMA-MA Blends

Material	E_a (kJ/mol)
SAN	189
SAN/MMA-MA0HMW	257
SAN/MMA-MA1HMW	258
SAN/MMA-MA5HMW	210
SAN/MMA-MA10HMW	225
SAN/MMA-MA1MMW	241
SAN/MMA-MA5MMW	202
SAN/MMA-MA10MMW	240
SAN/MMA-MA1LMW	248
SAN/MMA-MA5LMW	295
SAN/MMA-MA10LMW	209

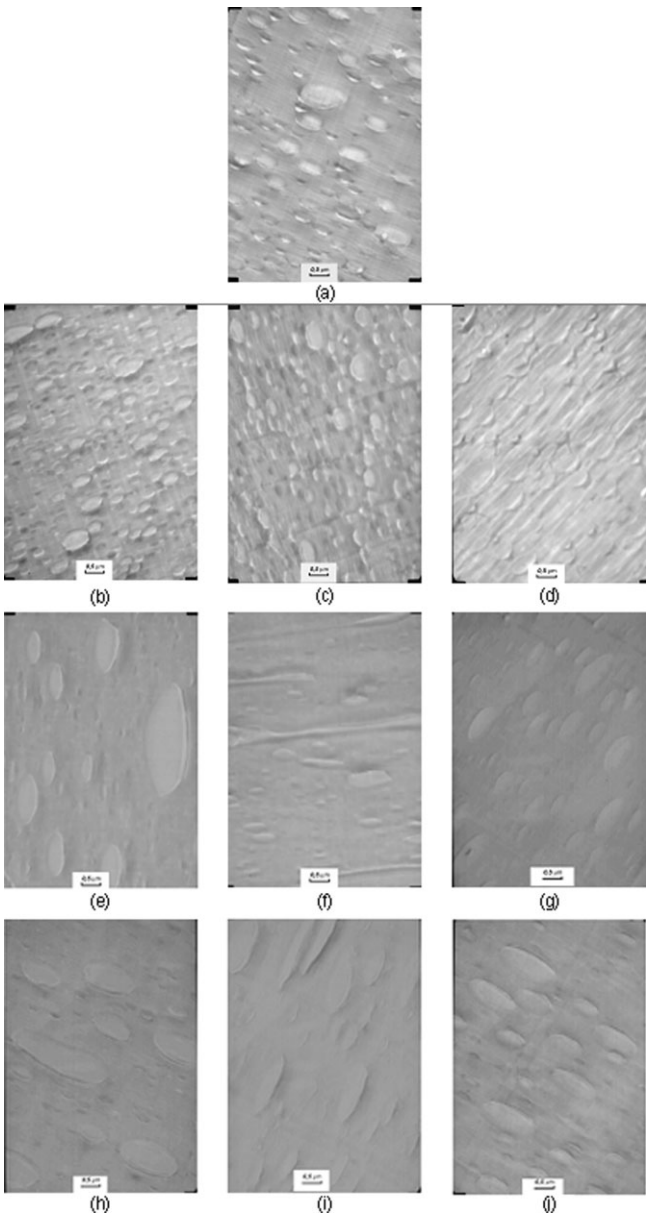

Figure 5 TEM Micrographies of the injection-molded blends: (a) PA/SAN; (b) aPA/SAN/MMA-MA1 HMW; (c) aPA/SAN/MMA-MA1 MMW; (d) aPA/SAN/MMA-MA1 LMW; (e) aPA/SAN/MMA-MA5 HMW; (f) aPA/SAN/MMA-MA5 MMW; (g) aPA/SAN/MMA-MA 5 LMW; (h) aPA/SAN/MMA-MA10 HMW; (i) aPA/SAN/MMA-MA10 MMW; and (j) aPA/SAN/MMA-MA10 LMW.

size, as shown in Figure 5(b–d). Therefore, the decrease in the SAN particle size when MMA-MA1 is added might correlates with the hypothesis of formation of aPA-*g*-MMA-MA grafted copolymers *in situ* at the interface. In addition, when MMA-MA copolymers containing 5% and 10% of maleic anhydride (MA) were added to the system, larger SAN particles size were observed [Fig. 5 (e) through (j)], which can be related to the coalescence phenomena. Another observation is that changes in the MMA-MA1 average molecular weight do not cause any significant change in the SAN particle size. It would be expected that lower molecular species (MMA-MA1 LMW) would have higher mobility to diffuse to the aPA/SAN blend interfase, thereby leading to higher emulsification efficiency. The effect of the amount of MA content in the MMA-MA copolymer as well as of the change in the molecular weight in the SAN particle size, can also be observed in Figure 6.

In the system aPA/SAN without the MMA-MA copolymer, the average diameter of the SAN particle size observed was about 0.18 μm. On the other hand, when the MMA-MA1 copolymer was added to the blend, the average particle size diameter decreased to 0.13 μm. The molecular weight of the compatibilizer did not show significant effect on the SAN particle size, within the molecular weight range used in this study. However, the addition of MMA-MA5 to MMA-MA10 copolymers to the aPA/SAN blends lead to a large increase in the SAN particle size, as observed in Figure 5. According to previous studies, it was expected that higher MA content in the MMA-MA copolymer would lead to systems with a finer morphology with smaller SAN particles. Majumdar and coworkers[25] have reported some insights about why that prediction is not always experimentally found. The maleic anhydride copolymer might react with end groups of the polyamide chain and become chemically bonded to the PA phase, whereas the MMA copolymer moieties are only physically bonded to the SAN phase. During the processing of these blends in the melt state, high shear stresses might remove the MMA-MA backbone of the graft copolymer from the SAN phase. The chemical reactions with amine end groups of

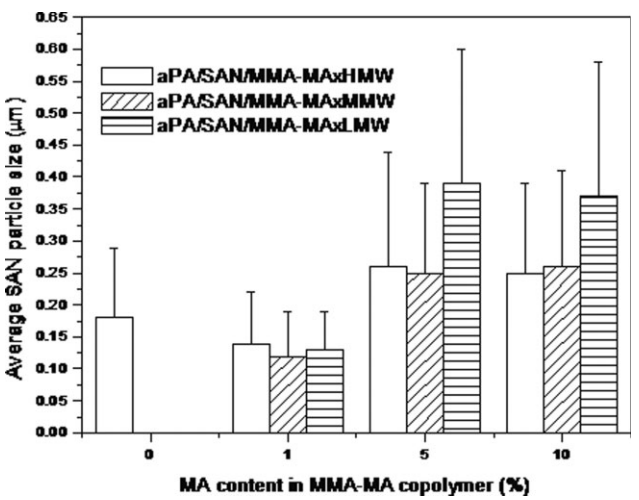

Figure 6 Average diameter of the disperse phase in aPA/SAN/MMA-MA blends as function of MA content in MMA-MA copolymer.

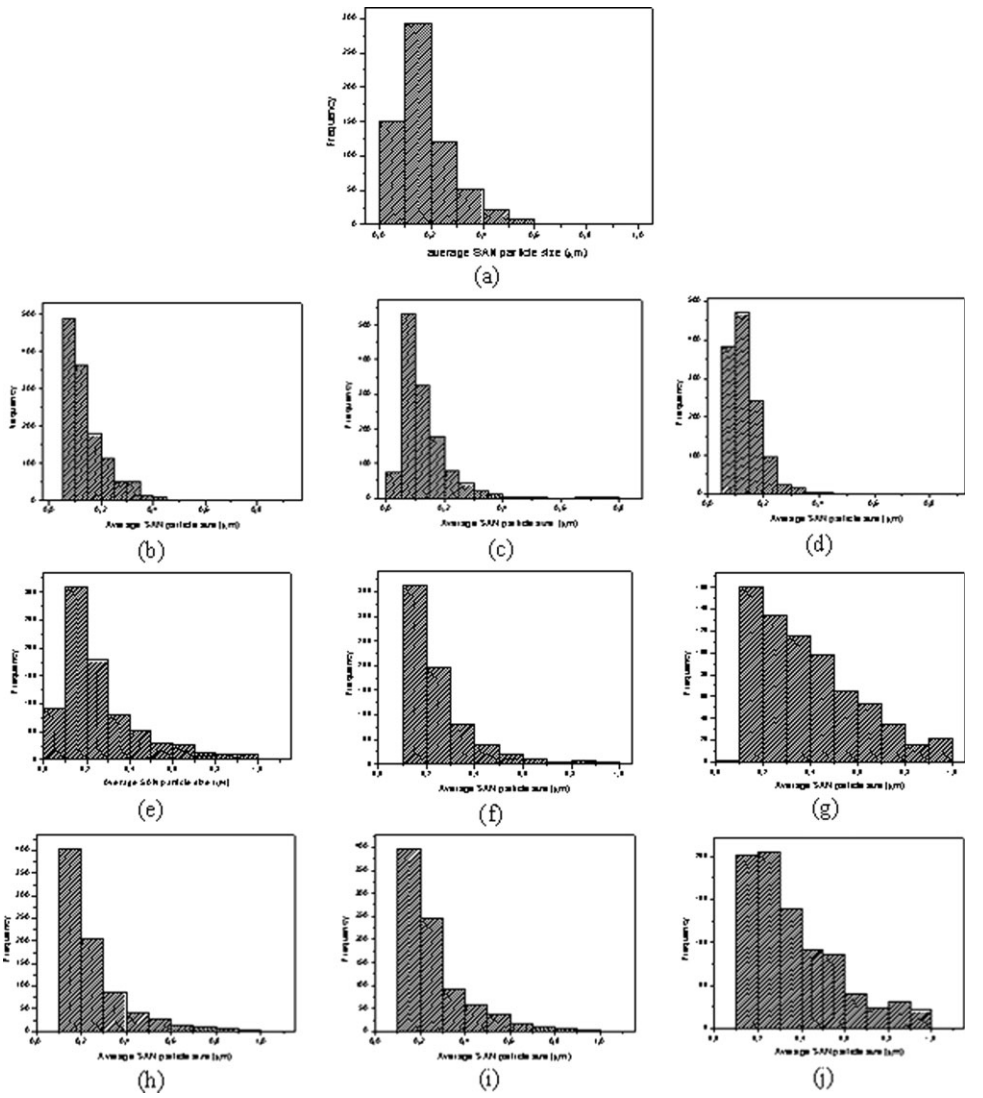

Figure 7 Histograms of particle size and distribution of particle size for the injected blends studied: (a) aPA/SAN; (b) aPA/SAN-MMA-MA1 HMW; (c) aPA/SAN/MMA-MA1 MMW; (d) aPA/SAN/MMA-MA1 LMW; (e) aPA/SAN/MMA-MA5 HMW; (f) aPA/SAN/MMA-MA5 MMW; (g) aPA/SAN/MMA-MA5 LMW; (h) aPA/SAN/MMA-MA10 HMW; (i) aPA/SAN/MMA-MA10 MMW; and (j) aPA/SAN/MMA-MA10 LMW.

the polyamide changes the chemical characteristics of the MMA-MA copolymer and at high extend of reaction the MMA-MA copolymer might became immiscible in the SAN phase. If the graft copolymer is removed from aPA/SAN interfase under the high stresses during processing, the surface of the dispersed phase particles will became with significantly depleted coverage which makes them more susceptible to coalescence. The confirmation of this inference is possible through the examination of the domain size distribution by observing the histogram shown in Figure 7. If high shear stress removes the backbones of the grafted copolymer from the interfase region, one could expect to observe domains of the graft copolymer in the a-PA matrix. Besides this, due to the chemical linkage, the domain size of the graft copolymer in the aPA matrix must be smaller than 100 nm. This is exactly what is observed in Figure 7 which confirms the hypothesis above.

Figure 8 shows a correlation between the extent of reaction between aPA amine end groups and the MA groups in the MMA-MA copolymers and the SAN dispersed phase particle size as function of MA content in MMA-MA copolymer. For the samples containing higher molecular weight MMA-MA copolymer, the amount of unreacted amine end groups decreases as the MA content increases [Fig. 8(a)]. As the MMA-MA molecular weight decreases, the amount of unreacted amine end groups reaches the lowest value as the MA content increases in the MMA-MA copolymer [Fig. 8(b,c)]. For the MMA-MA grade with the lower molecular weight, the lowest unreacted amine end groups limit is reached for the MMA-MA containing 1% of MA, as result of its

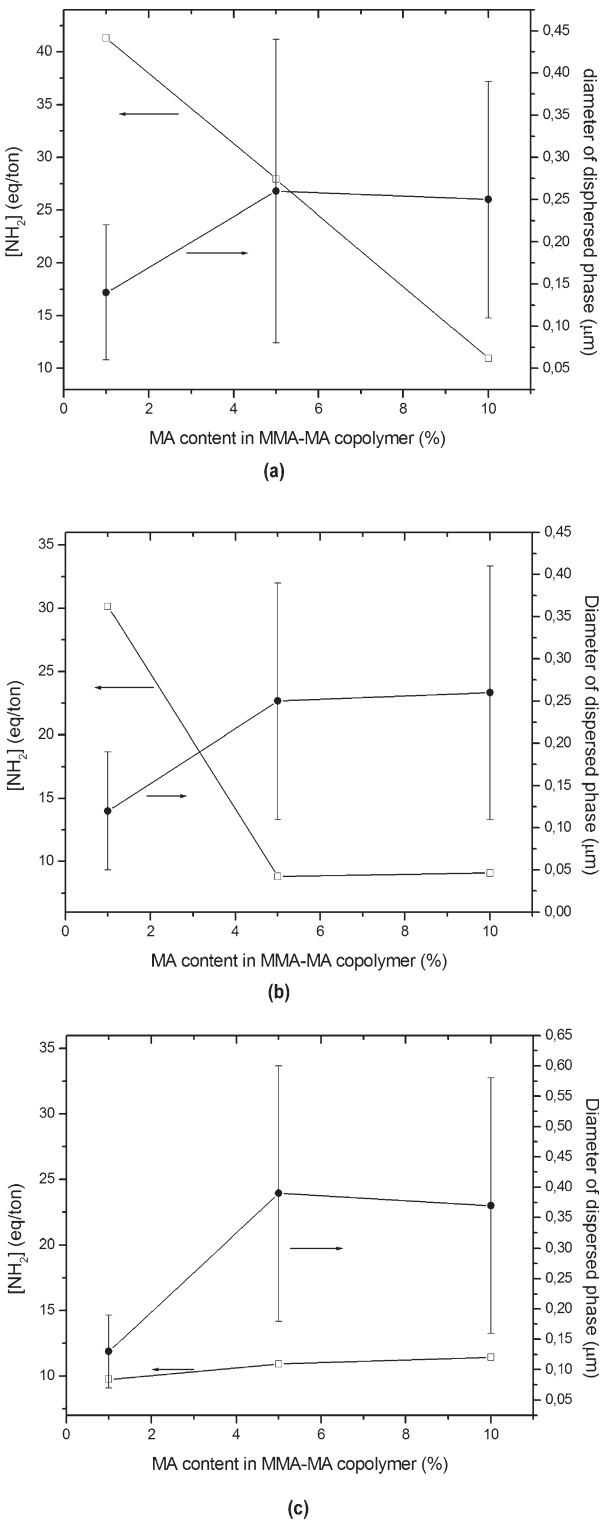

Figure 8 Unreacted amine end groups content and dispersed phase particle size as function of MA content in MMA-MA copolymer for aPA/SAN/MMA-MA blends for different MMA-MA molecular weight: (a) MMA-MA high-molecular-weight (HMW); (b) MMA-MA medium-molecular-weight (MMW); and (c) MMA-MA lower molecular weight (LMW). The solid lines between data points are for eye guiding purpose only.

higher molecular mobility during melt mixing. Although the amount of unreacted amine end groups has changed, the same trend between SAN particle size and MMA-MA molecular weight grade was observed.

It is also interesting to observe that reactively compatibilized blends may have a significantly higher melt viscosity than their uncompatibilized counterparts due to the grafting reaction which can alter the viscosity ratio between the disperse phase and the polymer matrix.[30,31] It is known that at low-viscosity-ratios, the disperse phase drop is highly deformed but do not break.[32] Table IV shows the torque values for all samples and the torque ratio for all SAN/(aPA-g-MMA-MA) systems, measured at 2 min of mixing. This mixing time was chosen because the residence time during the blend preparation by extrusion is similar to this time span. It can be observed that the addition of MMA-MA copolymer with higher level of MA to the aPA/SAN blends lead to a reduction in the torque ratio. Wu[33] has shown that the smallest particle size for uncompatibilized blends is reached when the viscosity ratio is ~ 1. Low-viscosity-ratio for the blend components SAN/(aPA-g-MMA-MA) would lead to poor dispersion of SAN domains in the aPA-rich matrix phase. Although torque measurements do not represent exactly the viscosity ratio for a given polymer system, a processing condition where the torque ratio approach 1 is the condition where the best dispersion is usually obtained. As the torque ratio becomes smaller than 1, the SAN particle size would increase in diameter as observed in Figure 6. On the other hand, the compatibilization effects is expected to reduce the interfacial tension, which would lead to smaller SAN particle size. The addition of MMA-MA in the aPA/SAN blends leads to the observation of both aforementioned effects. The SAN particle

TABLE IV
Torque Values for aPA, San, and aPA/MMA-MA Materials and Torque Ratio for the SAN/(aPA/MMA-MA) Blends, Measured at 2 min, at 260°C and 60 rpm

Samples	Torque at 2 min (Nm)	Torque ratio [SAN/(aPA/MMA-MA)]
SAN	1.9	–
aPA	2.4	0.8
aPA/MMA-MA1HMW	3.7	0.5
aPA/MMA-MA5HMW	3.8	0.5
aPA/MMA-MA10HMW	3.7	0.5
aPA/MMA-MA1MMW	6.5	0.3
aPA/MMA-MA5MMW	10.0	0.2
aPA/MMA-MA10MMW	8.3	0.2
aPA/MMA-MA1LMW	9.2	0.2
aPA/MMA-MA5LMW	11.2	0.2
aPA/MMA-MA10LMW	9.2	0.2

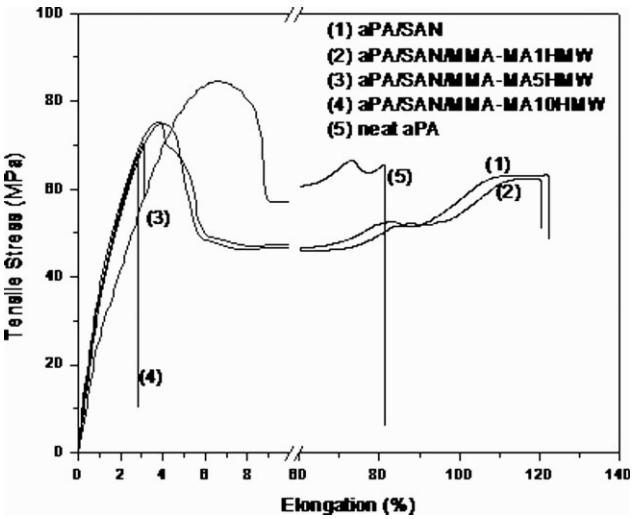

Figure 9 Stress–strain curves for aPA/SAN/MMA-MAxHMW blends studied.

size increases as the torque ratio is well below 1, but still remain very small in the range of 0.1 to 0.6 μm. Addition of the low-molecular-weight MMA-MA copolymers to the aPA/SAN blends promoted more significant increase in the SAN average particle size. The higher mobility of lower MW copolymers may lead to larger extend of grafting reactions within the residence time of $\sim$ 2 min within the extruder. This hypothesis is in agreement with the observations through the torque values (Table III). It has to be considered in this analysis that the SAN particle size do not show a very clear trend due to the addition of the different MMA-MA copolymers mainly because the particle size distributions are quite wide for most of the samples studied as observed through the error bars in Figure 6. As can be observed in Figure 5, the disperse phase domains in the blends with compatibilizer with high MA content shows orientation along the shear direction indicating that these blends have significantly higher melt viscosity when compared with similar systems without the compatibilizer. The results observed indicate that the viscosity ratio plays a very important role in the morphology formation for the aPA/SAN blends studied.

Tensile properties

The amorphous polyamides show ductile behavior under standard tensile testing, whereas SAN materials are essentially brittle and break before yielding.[34] On the other hand, the aPA/SAN blends may show both behaviors, depending on their morphology. The tensile test curves for the binary aPA/SAN and the ternary aPA/SAN/MMA-MA blends can be observed in the Figure 9. The presence of very small SAN particles (Fig. 5) seems to correlate with the ductile behavior for the aPA/SAN and aPA/SAN/MMA-MA1 HMW blends. The blends without the addition of MMA-MA and with MMA-MA containing 1% of MA shows very significant plastic deformation. Addition of MMA-MA copolymer with high-molecular-weight and high MA content leads the aPA/SAN blends to show a brittle behavior. We speculate that the addition of MMA-MA copolymers with high MA content leads not only to the formation of large SAN disperse particles but also it promotes the embrittlement of the aPA matrix due to more intense *in situ* grafting and possibly some crosslinking reactions, as discussed earlier.

Table V summarizes the results for tensile tests obtained for all samples studied. The values of the tensile yield stress are reduced by the addition of SAN when compared with the value for neat aPA. On the other hand, the addition of SAN and MMA-MA to aPA leads to an increased in the tensile modulus for the blends compared with aPA value or to values comparable to the modulus of the SAN. The ductility of the materials as observed through the results of elongation at break and the area under

TABLE V
Effect of MA Content at MMA-MA and MMA-MA Molecular Weight on Tensile Properties

Materials and blends	Yield strength (MPa)	Tensile modulus (GPa)	Elongation at break (%)	Area under tensile curves (MPa × mm/mm)
aPA	84 ± 0.5	2.9 ± 0.1	78 ± 6	46.7 ± 3.9
SAN	–	3.7 ± 0.5	3.1 ± 0.3	1.3 ± 0.1
aPA/SAN	76 ± 1.5	3.7 ± 0.3	125 ± 18	70.0 ± 4.6
aPA/SAN/MMA1 HMW	75 ± 0.9	3.8 ± 0.3	129 ± 7	65.4 ± 4.1
aPA/SAN/MMA1 MMW	77 ± 0.9	3.6 ± 0.4	52 ± 38	30.5 ± 15.4
aPA/SAN/MMA1 LMW	76 ± 0.7	3.5 ± 0.2	153 ± 20	88.0 ± 4.1
aPA/SAN/MMA5 HMW	–	3.6 ± 0.1	3.4 ± 0.2	2.6 ± 2.2
aPA/SAN/MMA5 MMW	–	3.4 ± 0.1	2.9 ± 0.4	1.2 ± 0.27
aPA/SAN/MMA5 LMW	–	3.6 ± 0.5	3.5 ± 0.7	1.7 ± 0.3
aPA/SAN/MMA10 HMW	–	3.9 ± 0.6	3.3 ± 0.2	1.5 ± 0.1
aPA/SAN/MMA10 MMW	–	3.5 ± 0.1	3.6 ± 0.1	1.7 ± 0.1
aPA/SAN/MMA10 LMW	–	3.5 ± 0.2	3.0 ± 0.2	1.2 ± 0.1

the tensile curves shows that the presence of SAN in the aPA matrix improves significantly both parameters. Addition of low MA content MMA-MA copolymer to the aPA/SAN does not change the high ductility of these blends. However, all the other blends containing MMA-MA with higher MA content have shown higher tensile modulus, lower elongation at break, and similar brittle behavior as the neat SAN. The higher toughness observed for the binary and for some of the ternary blends may be due to the corresponding morphology with a very fine dispersion of SAN-rich phase in the aPA matrix. It is well known that an appropriate disperse phase with an optimal particle size might improve a polymer matrix toughness as a result of local stress concentration around the particles and its ability for energy absorption through crazing and/or shear yielding deformation mechanisms.[35] Although polymer toughness improvement is more usually obtained through addition of rubber disperse phase to a brittle matrix, different kinds of disperse phase may trigger the aforementioned toughening mechanisms. The molecular weight of the compatibilizer seems to affects the ductility of the aPA/SAN/MMA-MA1 blends. The addition of medium-molecular-weight MMA-MA copolymer (MMA-MA1 MMW) to the blends lead to lower elongation at break and smaller area under the stress–strain curves. It was not found a reasonable explanation for this result once although the SAN's particle size for this system seems to be smaller than for the other blends, as shown in Figure 5(c), the corresponding SAN particle size distribution was not very different from the system using higher and lower molecular weight MMA-MA1 components, as shown in Figure 6. The tensile modulus for these blends are essentially independent of the MA content and of the MMA-MA molecular weight within the limits used in this study.[33] The elongation at break for higher MA content in the MMA-MA copolymer does not change with variation in MA content and molecular weight of the copolymer. These results suggest that in the systems with compatibilizer with high MA content, the SAN phase affects the elongation at the break results due to the brittle nature of the dispersed phase.

CONCLUDING REMARKS

The aPA/SAN blends studied showed a very fine SAN dispersed phase due to similar melt viscosity during mixing. Evidences for *in situ* reactions during the aPA/SAN/MMA-MA blends preparation in the melt state were observed through increase in the torque values for aPA/MMA-MA blends prepared in an internal mixer and mainly by a reduction in the amine end group content in the blends of aPA with addition of the MMA-MA compatibilizer. The molecular weight and the chemical characteristics of the MMA-MA copolymer affect the dispersed particle size. The SAN phase improved the tensile modulus and the aPA ductility for the systems studied. Addition of MMA-MA copolymer with low MA content was more effective for the improvement of the mechanical properties of the aPA/SAN blends. On the other hand, addition of MMA-MA copolymer with high content of MA led to brittle aPA/SAN blends. The results shown that the viscosity ratio also plays a very important role in the morphology formation and consequently on the properties of the aPA/SAN blends studied.

The authors are grateful to Dupont and Dow Chemical for providing the aPA and SAN materials, respectively.

References

1. Paul, D. R.; Bucknall, C. B. Polymer Blends; Wiley: NY, 2000; Vol. 1.
2. Majumdar, B.; Keskkula, H.; Paul, D. R. Polymer 1994, 35, 3164.
3. Cho, K.; Seo, K. H.; Ahn, T. O.; Kim, J.; Kim, K. U. Polymer 1997, 38, 4825.
4. Jafari, S. H.; Pötschke, P.; Stephan, M.; Walth, H.; Alberts, H. Polymer 2002, 43, 6985.
5. Jafari, S. H.; Pötschke, P.; Stephan, M.; Pompe, G.; Warth, H.; Alberts, H. J Appl Polym Sci 2002, 84, 2753.
6. Larocca, N. M.; Hage, E., Jr.; Pessan, L. A. J Polym Sci Part B: Polym Phys 2005, 43, 1244.
7. Aoki, Y.; Watanabe, M. Polym Eng Sci 1992, 32, 878.
8. Misra, A.; Sawhney, G.; Ananda Kumar, R. J Appl Polym Sci 1993, 50, 1179.
9. Jang, S. P.; Kim, D. Polym Eng Sci 2000, 40, 1635.
10. Kudva, R. A.; Keskkula, H.; Paul, D. R. Polymer 2000, 41, 239.
11. Araújo, E. M.; Hage, E., Jr.; Carvalho, A. J. F. J App Polym Sci 2003, 87, 842.
12. Araújo, E. M.; Hage, E., Jr.; Carvalho, A. J. F. J Mater Sci 2003, 38, 3515.
13. Kudva, R. A.; Keskkula, H.; Paul, D. R. Polymer 1998, 39, 2447.
14. Kitayama, N.; Keskkula, H.; Paul, D. R. Polymer 2000, 41, 8041.
15. Kitayama, N.; Keskkula, H.; Paul, D. R. Polymer 2000, 41, 8053.
16. Majumdar, B.; Keskkula, H.; Paul, D. R. J Polym Sci Part B: Polym Phys 1994, 32, 2127.
17. Majumdar, B.; Keskkula, H.; Paul, D. R. Polymer 1994, 35, 5453.
18. Chiou, J. S.; Paul, D. R.; Balow, J. W. Polymer 1982, 23, 1543.
19. Chu, J. H.; Paul, D. R. Polymer 1999, 40, 2687.
20. Bassani, A. Ph.D. Thesis; Universidade Federal de São Carlos: São Carlos, Brazil, 2003.
21. Spridon, D.; Panaitecu, L.; Ursu, D.; Uglea, C. V.; Popa, I.; Ottenbrite, R. M. Polym Int 1997, 43, 175.
22. Popa, I.; Offenberg, H.; Beldie, C.; Uglea, C. V. Eur Polym J 1997, 33, 1511.
23. Wilde, M. C.; Smets, G. J Polym Sci 1950, 253.
24. Becker, O.; Simon, G. P.; Rieckmann, T.; Forsythe, R.; Rosu, R.; Völker, S.; O'shea, M. Polymer 2001, 42, 1921.

25. Majumdar, B.; Paul, D. R.; Oshinski, A. J. Polymer 1997, 38, 1787.
26. Sundararaj, U.; Macosko, C. W. Macromolecules 1995, 28, 2647.
27. Lepers, J. C.; Favis, B. D.; Lacroix, C. J Polym Sci Part B: Polym Phys 2001, 39, 601.
28. Wildes, G.; Keskkula, H.; Paul, D. R. J Polym Sci Part B: Polym Phys 1999, 37, 71.
29. Lyu, S. P.; Jones, T. D.; Bates, F. S.; Macosko, C. W. Macromolecules 2002, 35, 7845.
30. Triacca, V. J.; Ziaee, S.; Barlow, J. W.; Keskkula, H.; Paul, D. R. Polymer 1991, 32, 1401.
31. Oshinski, A. J.; Keskkula, H.; Paul, D. R. Polymer 1992, 33, 268.
32. Favis, B. D.; Chalifoux, J. P. Polym Eng Sci 1978, 27, 1591.
33. Wu, S. Polymer 1985, 26, 1855.
34. Kitayama, N.; Keskkula, H.; Paul, D. R. Polymer 2001, 42, 3751.
35. Bucknall, C. B. Toughened Plastics; Applied Science Publ.: London, 1977.